**Proceedings of the ASME 2019
Dynamic Systems and Controls Conference
DSCC2019
October 8-11, 2019, Park City, Utah, USA**

DSCC2019-9082

DESIGN AND CHARACTERIZATION OF A PASSIVE INSTRUMENTED HAND

Saad N. Yousaf[1], Victoria S. Joshi[1], John E. Britt[1], Chad G. Rose[2], and Marcia K. O'Malley[1]
[1] Mechatronics and Haptic Interfaces Laboratory, Department of Mechanical Engineering, Rice University, Houston, TX
[2] ReNeu Robotics Lab, Department of Mechanical Engineering, University of Texas at Austin, Austin, TX
Email: chadgrose@utexas.edu

ABSTRACT

Although soft robotic assistive gloves have high potential for restoring functional independence for individuals with motor impairment, their lack of rigid components makes it difficult to obtain accurate position sensing to validate their performance. To track soft device motion, standard practice rely on costly optical motion capture techniques, which have reduced accuracy due to limitations in marker occlusion and device deformation. We propose the Instrumented Hand as a low-cost, open-source measurement tool to serve as a standard solution for comparing joint-level position and torque measurements from magnetoresistive sensors. Shown in a case study, the Instrumented Hand can be used to validate soft wearable devices and evaluate range of motion (ROM) and torque capabilities.

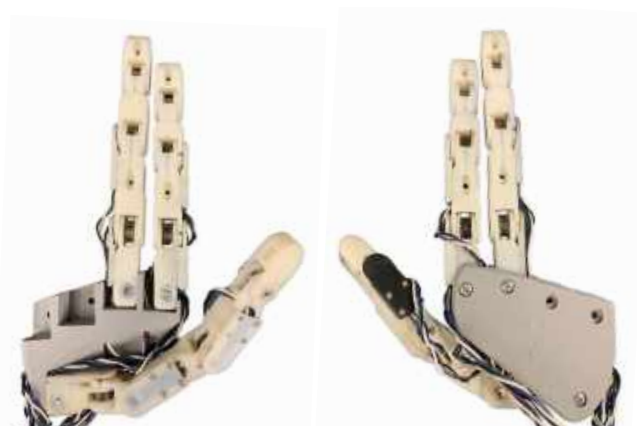

FIGURE 1. The open-sourced Instrumented Hand for soft device validation measures joint level information from the thumb, index, and middle fingers. Palmar side (left) and dorsal side (right).

INTRODUCTION

Due to neuromuscular injuries or disorders, a large population suffers from reduced upper extremity motor function. Of the 6.6 million Americans with stroke and the 5.3 million with traumatic brain injuries, a significant number have hand impairments that prevent unassisted completion of Activities of Daily Living (ADLs), reducing their quality of life (QOL) [1,2]. Furthermore, over half of 17,000 annual cases of spinal cord injury occur at the cervical level and thus result in severe disabilities in an individual's upper extremities [3].

Unlike their rigid counterparts, which are generally too heavy, non-compliant, and stationary to be used effectively for a long period of time [4], soft robotic assistive gloves have the potential to restore functional independence to individuals with motor impairment and improve their QOL. The flexible nature of these gloves inherently removes potentially harmful constraints between non-actuated joints and allows for conformation to the curves of the human body [5]. However, soft device validation presents challenges because they can only operate by applying reaction forces to a substrate (the wearer's hand). Ensuring that the hand used in validations is of a standard size and remains passive is difficult to demonstrate. Validating the range of motion (ROM) and accuracy of position sensing is especially important for wearable hand devices because they must achieve high performance in joint ROM and finger positioning to allow the user to perform ADLs.

Soft device validation currently has two obstacles which have yet to be addressed. First, there are currently no hand mannequins available that facilitate the accurate testing of a soft robotic hand device. Existing hand models used for studying human hand motion, such as the Anatomically Correct Testbed Hand [6] or prosthetic hands, are actuated and therefore generally not backdrivable, which would interfere with the validation process. The non-actuated models that are commercially available, such as Ikea's Handskalad [7], the Dapper Cadaver's realistic-looking posable models [8], or Anthromod's 3D Printable Right Hand [9], lack realistic joint motion that would replicate a human thumb's motion, and are not readily modifiable to accommodate position sensors that would be useful for determining ROM.

Furthermore, the standard method of using optical motion capture to validate wearable devices relies on expensive equipment which still suffers from a range of limitations [10]. First and foremost is the cost, both in terms of purchasing the equipment and in terms of set up time. Marker occlusion also becomes problematic, since the hand requires a large number of markers in close proximity with one another. Lastly, it is difficult to prevent motion of the skin relative to the muscle/bone structure underneath, or relative motion of the soft device with respect to the wearer. Both of these issues can result in measurement noise or inaccuracies which reduce the usefulness of motion capture. A solution which overcomes these challenges stands to both improve device validation as well as democratize the field of device design.

Previous attempts have been made to create such a solution in the form of an instrumented finger, but even these efforts have limitations. The open-source testbed finger [11] developed by Yun *et al.* is too large to fit inside a standard-sized glove [12], so it is not useful for testing a significant number of wearable devices. The instrumented finger developed by Rose *et al.* [13, 14] is small enough to fit into a glove, but it is not connected to a palm or any other fingers, preventing necessary multi-fingered grasp testing.

Thus, the low-cost, open-source Instrumented Hand shown in Fig. 1 is proposed as a standard solution for designers of wearable hand devices to compare ROM and torque control between various devices and actuation methods. With instrumented joints and reasonably accurate thumb joint motion, the Instrumented Hand has the potential to replace expensive motion capture and provide known interaction forces for wearable devices, moving a step towards a standard, open-sourced mannequin with reasonably accurate thumb motion that can easily enable comparisons across projects and inspire better device design.

This manuscript introduces the design and manufacturing of the Instrumented Hand testbed as well as its mechanical properties and instrumentation. A case study demonstrating the performance of the mannequin with a soft device is also presented. The results of this case study and the discussion of the future improvements conclude the manuscript.

DESIGN AND FABRICATION

The mechanical design of the Instrumented Hand is driven by its intended use with soft wearable hand devices. Design criteria include accurate measurement of joint angles, ease of fit within the wearable device, and ease of open-sourcing the solution. Able-bodied ROM for the metacarpophalangeal (MCP), proximal interphalangeal (PIP), and distal interphalangeal (DIP) joints is 100°, 105°, and 85°, respectively [15]. The Instrumented Hand supports more than 120°of rotation for both the MCP and PIP joints.

The Instrumented Hand approximates human finger joint motion with rotary pin joints, based on studies showing that the complex motion of the finger joints can be modeled as rotary joints with little loss of accuracy [16, 17]. As shown in Fig. 2, only the thumb consisting of the carpometacarpal (CMC), MCP, and interphalangeal (IP) joints), index, and middle fingers are instrumented since they are the basis for dexterous hand grasps. Tendon-driven devices such as the PolyGlove [18], the Exo-Glove [19], the glove by Xiloyannis *et al.* [20, 21] and the J-Glove [22] support only a single three finger grasp. Other rigid hand exoskeletons such as the Maestro [4] also focus on three finger actuation.

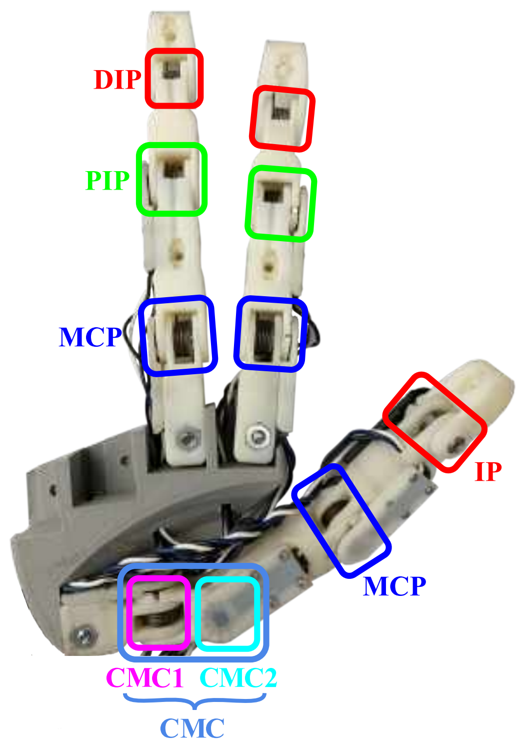

FIGURE 2. The Instrumented Hand with all rotary joints labelled. The CMC joint is approximated by two rotary joints, CMC1 and CMC2. The link between the thumb CMC and MCP joints is rotated to enable a more natural thumb orientation and flexion motion.

FIGURE 3. Side view of the PIP and DIP joints on the instrumented finger show the 1:1 coupling achieved by using a kevlar braided line (1 mm, Spear-It) as highlighted in green and anchored on either end.

Each finger on the Instrumented Hand has flexion and extension at the MCP, PIP, and DIP joints. The DIP and PIP joints are coupled with a biologically-inspired tendon, following the path shown in Fig. 3. To capture the complexity of motions at the CPC joint, two orthogonal pin joints are designed next to each other with CPC1 capturing opposition, and CPC2 capturing flexion and extension. A ball-and-socket joint was not pursued due to limitations in sensing the motion of such a configuration. The MCP and IP thumb joints also aid in thumb flexion and extension. The thumb metacarpal phalanx between the CPC and the MCP joints in the Instrumented Hand twists 45° to achieve a flexion direction representative of the human thumb. Overall, the Instrumented Hand's thumb allows for flexion and extension as well as opposition/reposition.

Each rotary joint on the Instrumented Hand consists of a 1/8" diameter shoulder bolt with a nut, two flanged bearings, a torsional spring, and a spacer between the spring and the shoulder bolt as shown on in Fig. 4(a). The springs provide a known restoring torque to joints, adding the potential of joint torque measurement. The springs at the CPC, MCP, and PIP joints (McMaster-Carr 9271K142) provide a maximum torque of 1.071 in-lbs. The smaller springs at the DIP joints (McMaster-Carr 9271K607) provide a maximum torque of 0.88 in-lbs. In each instrumented joint, the nut side of the outer phalange holds a ring neodymium magnet and a cover holds the magnetoresistive angle sensor, shown in Fig. 4(b).

The fingers and thumb attach to a central palm piece. Each finger's links are anthropometrically sized and bolted to the palm. The fingers are designed to be slightly abducted to present a natural hand pose. The abduction/adduction of each finger can be slightly adjusted behind the MCP joint. The palm also serves as a wire routing pathway for wires to the sensors. The current design of the palm is also driven by the size criteria as it plays a crucial role in determining how the Instrumented Hand fits inside wearable devices. Most components are 3D printed (Objet RGD 450) to reduce cost and fabrication time.

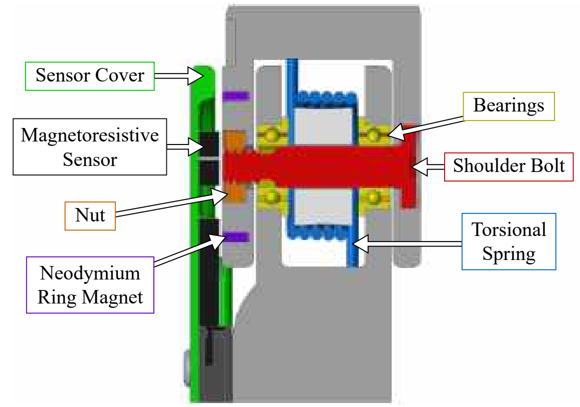

(a) Section View

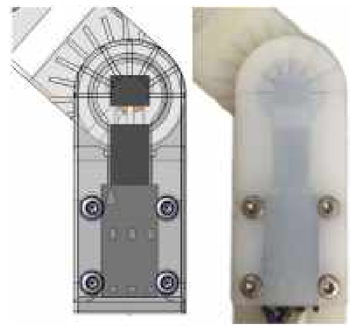

(b) Side View

FIGURE 4. (a) Cross sectional view of a rotary joint showing the sensor cover (green), magnetoresistive sensor (black), neodymium ring magnet (purple), nut (orange), bearings (yellow), shoulder bolt (red), and torsional spring (blue). (b) Side views of a rotary joint showing the indentations used to visually measure joint angles at 15° increments for calibration. The sensor cover assembly is also shown.

JOINT INSTRUMENTATION

Magnetoresistive linear angle sensors (KMA210) with neodymium ring magnets are used to measure the angular position for each joint which is instrumented. There are eight total sensors on the current Instrumented Hand. The thumb has sensors at the CPC1, CPC2, MCP, and IP joints. The index and middle fingers also have sensors at the MCP and PIP joints. The layout of joints can be seen in Fig. 2. A cover holds the magnetoresistive sensor in place alongside each joint to rigidly anchor the sensor as the neodymium ring magnet rotates with joint motion. Fig. 4(b) shows the sensor setup. The magnetic orientation determines the voltage output from the sensor, which is measured by a Quanser Q8-USB DAQ. The measurements are processed through C++ code that based on the Mechatronics Engine and Library [23].

To obtain accurate angle readings from the magnetoresistive sensor, it is necessary to calibrate each joint due to factors that arise during assembly, such as variations in magnet orientation and distance between the magnet and sensor. Each joint on the thumb is marked at 30° intervals to provide a visual cue for the joint's rotation. Each joint on the other fingers is marked at 15° intervals for more precise measurement, as seen in Fig. 4(b).

During initial calibration testing, significant magnetic interference was observed between the sensors on the index and middle fingers. As a solution, the sensors and magnets were placed on the opposite sides of each finger to create space between the magnets. This significantly reduced magnetic interference and provided more accurate angle readings.

INSTRUMENTED HAND CHARACTERIZATION

To determine the accuracy of joint angle measurements with the Instrumented Hand, sensor outputs were compared to ground-truth measures. First, average sensor voltage measurements were recorded at 15° increments from 0° to 90° for the index and middle finger joints and 30°increments for the thumb joints to create a linear regression to accurately provide joint angle based on sensor readings. An example calibration is illustrated in Fig. 5. The corresponding R^2 values of the linear regressions for each joint are given in Table 1. Then, mechanical jigs were laser cut at the same 15° intervals as the calibration angles and compared to the Instrumented Hand measurements. For each joint, one end was clamped and the jigs were used to hold the joint. The measured angle for ten samples was averaged and compared to the known angle from the jig. The maximum error for each joint angle measurement is shown in Table 1. All joint angles were accurately measured within 7°.

Further testing was conducted to characterize joint torques on the Instrumented Hand given known joint angles and specifications for the torsional spring. The testing configuration is shown in Fig. 6(a), in which one phalanx was clamped at 0° horizontally and the next phalanx was loaded with a hanging weight. The joint was thus subjected to a torque as weight was loaded and unloaded, with a torque relationship given by Eq. 1. Each set of loading and unloading was conducted three times. The middle finger's MCP joint was used for testing, but the same mechanics apply to seven out of eight joints on the Instrumented Hand (thumb IP uses a different spring).

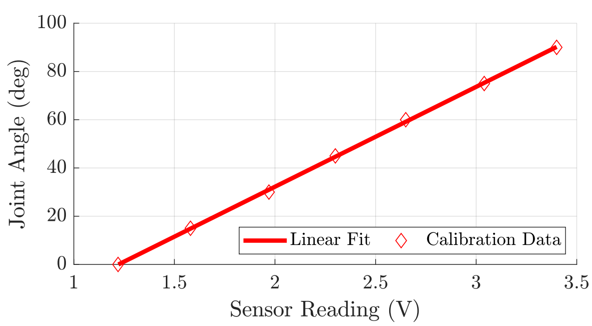

FIGURE 5. Calibration data from the PIP joint on the index finger with a linear regression ($R^2 = 1$), representative of all joints. As expected, the highly linear output for each of the joints of the Instrumented Hand supports its use in experimental validation of soft hand exoskeletons.

TABLE 1. DEVICE CHARACTERIZATION OF THE JOINT MEASUREMENT CAPABILITIES OF THE INSTRUMENTED HAND.

Joint	R^2	Max Error
Thumb CPC1	0.997	5.55°
Thumb CPC2	0.982	5.35°
Thumb MCP	0.988	6.27°
Thumb IP	0.996	6.26°
Index MCP	0.999	2.93°
Index PIP	1	2.40°
Middle MCP	0.999	4.95°
Middle PIP	1	2.01°

$$\tau = R * (W cos(\theta)) = \kappa\theta \qquad (1)$$

The torque measurement characterization results are shown in Fig. 6(b). Compared to the expected torque curve based on the torsional spring coefficient (0.0005378 N-m/°), the joint torque curve is lower due to losses from friction. Specifically, there is approximately a 20% loss observed. The R^2 value for joint torque versus joint angle is 0.942, and the maximum 95% confidence interval is 0.0104 N-m (at the end of the ROM).

CASE STUDY: SPAR GLOVE

As a case study, the Instrumented Hand was used to determine the range of motion and the quality of measurement of the sensors in the SeptaPose Assistive and Rehabilitative (SPAR) Glove [14], a semi-soft device which actuates the thumb, index, and middle fingers. The Instrumented Hand was placed in the SPAR Glove with an uninstrumented ring finger as well as padding on the palm to simulate the thenar and hypothenar eminences. For testing purposes, the SPAR Glove was held such that motion was not in the plane of gravity. Data were gathered as the SPAR Glove was actuated between the two hand poses shown in Fig. 8(a), and (b), reposition and lateral pinch, respectively. Data were collected from the Instrumented Hand joints as well as from linear position

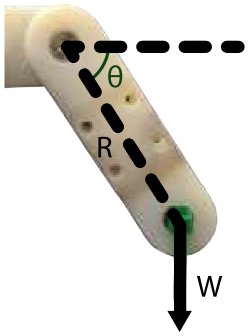

(a) Torque Characterization Method

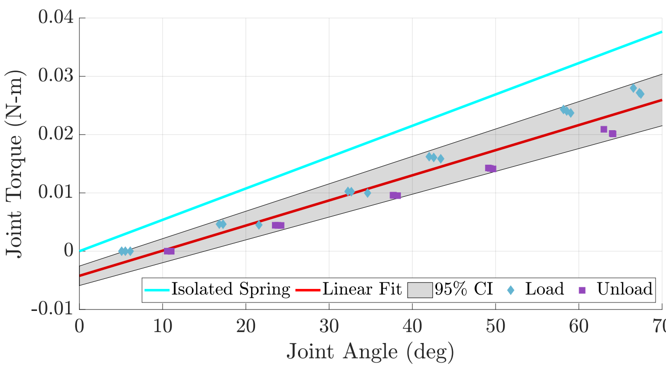

(b) Torque Characterization Results

FIGURE 6. (a) Testing configuration for the joint torque measurement test, showing the joint angle measured and the weight loading. The attached weight provided a known force for determining the torque measurement capabilities of the Instrumented Hand. (b) Testing results showing the relationship between torque and joint angle with the 95% confidence interval possessing a width of .0104 N-m at the end of the ROM. The R^2 value for the linear fit shown in red is 0.9416. Also shown is the relationship for the spring in isolation based on manufacturer's specifications.

transducers (LPTs) integrated in the SPAR Glove. Fig. 8(c), (d), and (e) show results from the index finger, middle finger, and thumb, respectively. The SPAR Glove was actuated to the lateral pinch pose three times at approximately 6-20 seconds, 27-40 seconds, and 47-58 seconds. These trials show the ROM of the SPAR Glove for this configuration and the performance of the distal sensing integrated into the glove.

DISCUSSION

The Instrumented Hand, as validated by its characterization and case study with the SPAR Glove, is a useful tool for establishing the performance of soft hand devices. When the readings from the Instrumented Hand were measured against standard measurement jigs, they were found to be reasonably accurate, with all joint angles accurately measured within 7°, as seen in Table 1. The variation in performance likely results from two causes: 1) magnetic interference between joints (in particular, the thumb joints are located near each other) and 2) limitations in the design and implementation of the standard measurement jigs. In this manuscript, each of the eight tested joints are considered equally valuable for hand movement and device validation, but future revisions to the design could consider establishing and leveraging the relative importance of each joint to hand motion.

The Instrumented Hand also performs well in measuring the ROM of the SPAR Glove and provides accurate joint angle measurements from the index finger, middle finger, and thumb. Furthermore, the Instrumented Hand possesses the capability to provide joint torque data based on joint angle measurements. The device characterization and case study with the SPAR Glove show the potential of using the Instrumented Hand for device design and validation.

The test with SPAR Glove provides insight regarding actuation between poses. First, by testing more than a single finger (such as the test completed by Rose and O'Malley [14]), interactions between the fingers and the ROM of targeted grasps are able to be measured. Additionally, quantitative information can be gleaned for each finger. The lack of thumb motion as seen in Fig. 8(e) motivates further development in both devices, identifying a need in the SPAR Glove design to increase both flexion and extension, as well as suggesting a kinematic mismatch between the Instrumented Hand and the human thumb. Across the fingers, LPT data aligned well with the Instrumented Hand data as shown in Fig. 8(c) and (d). As ex-

FIGURE 7. The SeptaPose Assistive and Rehabilitative (SPAR) Glove with individually actuated thumb, index, and secondary fingers is a soft exoskeleton which relies on the wearer's musculoskeletal system for reaction forces. This reliance on a wearer makes the SPAR Glove a good candidate for validation with the Instrumented Hand. Figure reproduced from [14].

(a) Reposition (b) Lateral Pinch

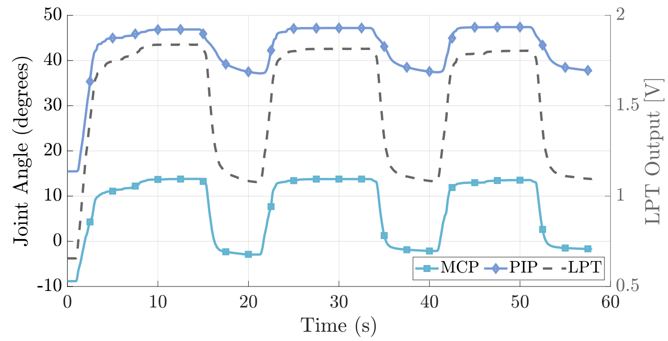

(c) Index Joint Angles

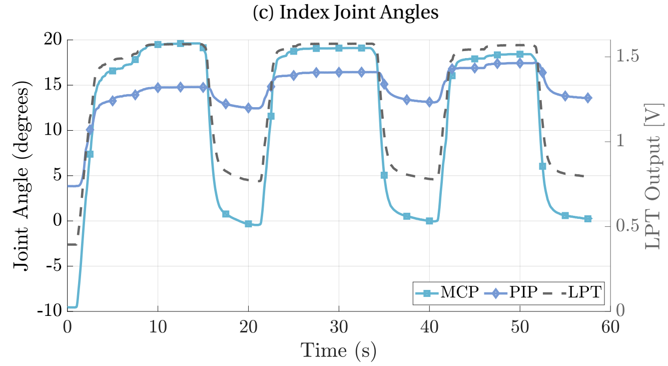

(d) Middle Joint Angles

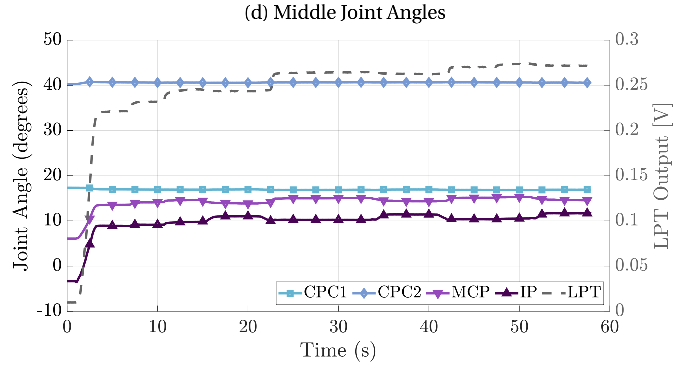

(e) Thumb Joint Angles

FIGURE 8. Two poses were commanded to the SPAR Glove and measured by the Instrumented Hand, (a) the reposition pose and (b) the lateral pinch pose, both of which require actuation of the thumb, index, and middle fingers. The resulting position measurements from the Instrumented Hand and the SPAR Glove's string potentiometer are presented for the (c) index finger, (d) middle finger, and (e) thumb. These results suggest that both the SPAR Glove and the Instrumented Hand may need further design improvements.

pected, the LPTs were unable to determine joint-level motion characteristics, and are in their current configuration unable to differentiate thumb pose. These limitations are present in nearly all soft robotic devices, which need devices like the Instrumented Hand to build models and characterize their distal sensing capabilities.

These tests also suggest future work for the Instrumented Hand. First, the mechanical design of the Instrumented Hand should be modified to better match joint kinematics, particularly the thumb CMC joint, and the form factor of the palm. Further improvements to the sensor implementation should reduce magnetic interference between the joints and extend beyond just joint angle measurement. To improve the force measurement capabilities of the Instrumented Hand, friction should be reduced. Future testing should also characterize joint torque information across the Instrumented Hand by testing multiple joints.

Ultimately, the use of the Instrumented Hand should be extended to other wearable hand devices for further testing. Further studies comparing the ROM estimated by the Instrumented Hand should be compared to studies with human participants to determine the relationship between a device's performance with the Instrumented Hand and human participants. In turn, new design insights can drive the development of a better Instrumented Hand.

CONCLUSION

Soft wearable robotic devices for the hand are being proposed which stand to restore or augment hand function for a wide population with hand impairment. These soft devices rely on the wearer's hand to provide reaction forces and guide the actuation to perform useful work. Separating the user's contribution to motion from the device's can be difficult. Further, soft device construction precludes measurement and device validations with traditional methods, instead relying on ad-hoc methods or expensive motion capture equipment. An Instrumented Hand has been proposed as a tool available to soft device designers which overcomes the limitations of other methods. With measurement capabilities and tunable mechanical properties, the Instrumented Hand can establish joint ROM and validate sensing strategies for a wide range of hand devices, as shown in a case study. The Instrumented Hand proposed in this manuscript serves as a first step towards a standard, open source tool for device designers.

ACKNOWLEDGMENT

We would like to thank Evan Pezent for his C++ wisdom, Zane Zook for his guidance on technical writing, and the Oshman Engineering Design Kitchen staff for their prototyping resources and expertise.

REFERENCES

[1] Mozaffarian, D., et al., 2016. "Executive summary: Heart disease and stroke statistics-2016 update: A report from the American Heart Association". *Circulation,* ***133***(4), pp. 447–454.

[2] Roozenbeek, B., Maas, A. I., and Menon, D. K., 2013. "Changing patterns in the epidemiology of traumatic brain injury". *Nature Reviews Neurology,* ***9***(4), pp. 231–236.

[3] National Spinal Cord Injury Statistical Center, 2016. "Spinal cord injury facts and figures at a glance". *Birmingham, AL: University of Alabama at Birmingham*.

[4] Yun, Y., Dancausse, S., Esmatloo, P., Serrato, A., Merring, C. A., Agarwal, P., and Deshpande, A. D., 2017. "Maestro: An EMG-Driven Assistive Hand Exoskeleton for Spinal Cord Injury Patients". In Robotics and Automation (ICRA), International Conference on, IEEE, pp. 2904–2910.

[5] Chu, C.-Y., and Patterson, R. M., 2018. "Soft robotic devices for hand rehabilitation and assistance: a narrative review". *Journal of NeuroEngineering and Rehabilitation,* ***15***(9).

[6] Deshpande, A. D., Xu, Z., Weghe, M. J. V., Brown, B. H., Ko, J., Chang, L. Y., Wilkinson, D. D., Bidic, S. M., and Matsuoka, Y., 2013. "Mechanisms of the anatomically correct testbed hand". *IEEE/ASME Transactions on Mechatronics,* ***18***(1), pp. 238–250.

[7] Inter IKEA Systems B.V. Handskalad. https://www.ikea.com/us/en/catalog/products/90424146. (accessed: 30.03.2019).

[8] Dapper Cadaver. Jamie hands. https://www.dappercadaver.com/products/jamie-hands?variant=10886936259. (accessed: 30.03.2019).

[9] Chappell, C., 2012. 3d printed hand right. https://www.shapeways.com/product/Z5CZ2RKLY/3d-printed-hand-right?optionId=42512474&li=marketplace. (accessed: 30.03.2019).

[10] Yun, Y., Agarwal, P., and Deshpande, A. D., 2014. "Accurate, robust, and real-time pose estimation of finger". *Journal of Dynamic Systems, Measurement, and Control,* ***137***(3), pp. 034505–1 – 034505–6.

[11] Yun, Y., Fox, J., Sarkar, S., and Deshpande, A. D., 2016. Testbed finger open source (UT_ReNeu_Archive). http://mahilab.rice.edu/content/open-source-instrumented-mannequins-wearable. (accessed: 30.03.2019).

[12] Yun, Y., Agarwal, P., Fox, J., Madden, K. E., and Deshpande, A. D., 2016. "Accurate torque control of finger joints with ut hand exoskeleton through bowden cable sea". In Intelligent Robots and Systems (IROS), International Conference on, IEEE, pp. 390–397.

[13] Rose, C. G., Juzswik, M., and O'Malley, M. K., 2018. Open-Source Instrumented Mannequins For Wearable Robots. http://mahilab.rice.edu/content/open-source-instrumented-mannequins-wearable. (accessed: 28.03.2019).

[14] Rose, C. G., and O'Malley, M. K., 2019. "Hybrid rigid-soft hand exoskeleton to assist functional dexterity". *IEEE Robotics and Automation Letters,* ***4***(1), pp. 73–80.

[15] Hume, M. C., Gellman, H., McKellop, H., and Brumfield Jr., R. H., 1990. "Functional range of motion of the joints of the hand". *The Journal of Hand Surgery,* ***15***(2), pp. 240–243.

[16] Rohling, R. N., and Hollerbach, J. M., 1993. "Calibrating the human hand for haptic interfaces". *Presence: Teleoperators and Virtual Environments,* ***2***(4), pp. 281–296.

[17] Griffin, W. B., Findley, R. P., Turner, M. L., and Cutkosky, M. R., 2000. "Calibration and mapping of a human hand for dexterous telemanipulation". In Haptic Interfaces for Virtual Environments and Teleoperator Systems Symposium, ASME IMECE 2000 Conference, ASME.

[18] Kang, B. B., Lee, H., In, H., Jeong, U., Chung, J., and Cho, K.-J., 2016. "Development of a polymer-based tendon-driven wearable robotic hand". In Robotics and Automation (ICRA), International Conference on, IEEE, pp. 3750–3755.

[19] In, H., Kang, B. B., Sin, M., and Cho, K.-J., 2015. "Exo-glove: A wearable robot for the hand with a soft tendon routing system". *IEEE Robotics & Automation Magazine,* ***22***(1), pp. 97–105.

[20] Xiloyannis, M., Cappello, L., Khanh, D. B., Yen, S.-C., and Masia, L., 2016. "Modelling and design of a synergy-based actuator for a tendon-driven soft robotic glove". In Biomedical Robotics and Biomechatronics (BioRob), International Conference on, pp. 1213–1219.

[21] Xiloyannis, M., Cappello, L., Binh, K. D., Antuvan, C. W., and Masia, L., 2017. "Preliminary design and control of a soft exosuit for assisting elbow movements and hand grasping in activities of daily living". *Journal of Rehabilitation and Assistive Technologies Engineering,* ***4***.

[22] Ochoa, J. M., Yicheng, J., Narasimhan, D., and Kamper, D. G., 2009. "Development of a portable actuated orthotic glove to facilitate gross extension of the digits for therapeutic training after stroke". In Engineering in Medicine and Biology Society, Annual International Conference of, IEEE.

[23] Pezent, E., and McDonald, C. G., 2019. Github - mahilab/MEL: Mechatronics Engine & Library. https://github.com/mahilab/MEL. (accessed: 18.01.2019).